Published in final edited form as:
Cancer Res. 2009 February 1; 69(3): 863–872. doi:10.1158/0008-5472.CAN-08-3057.

Loss of *Rad51c* leads to embryonic lethality and modulation of *Trp53*-dependent tumorigenesis in mice

Sergey G. Kuznetsov[1], **Diana C. Haines**[2], **Betty K. Martin**[1], and **Shyam K. Sharan**[1,*]

[1]Mouse Cancer Genetics Program, Center for Cancer Research, National Cancer Institute at Frederick, Frederick, Maryland 21702, U.S.A

[2]Pathology Histotechnology Laboratory, SAIC-Frederick, National Cancer Institute at Frederick, Frederick, Maryland 21702, U.S.A.

Abstract

RecA/Rad51 protein family members (Rad51, Rad51b, Rad51c, Rad51d, Xrcc2, and Xrcc3) are essential for DNA repair by homologous recombination and their role in cancers has been anticipated. Here we provide the first direct evidence for a tumor suppressor function for a member of the Rad51 family. We show that *Rad51c* deficiency leads to early embryonic lethality, which can be delayed on a *Trp53-null* background. To uncover the role of *Rad51c* in tumorigenesis, we have exploited the fact that *Rad51c* and *Trp53* are both closely located on the mouse chromosome 11. We have generated double heterozygous (*DH*) mice carrying mutant alleles of both genes either on different (*DH-trans*) or on the same chromosome (*DH-cis*), the latter allowing for a deletion of wild-type alleles of both genes by loss of heterozygosity (LOH). *DH-trans* mice, in contrast to *DH-cis*, developed tumors with latency and spectrum similar to *Trp53* heterozygous mice. Strikingly, *Rad51c* mutation in *DH-cis* mice promoted the development of tumors of specialized sebaceous glands and suppressed tumors characteristic of *Trp53* mutation. In addition, *DH-cis*, females developed tumors significantly earlier than any other group.

Keywords

Rad51c; knockout mice; preputial gland; Rad51 paralogs; sebaceous tumor; *Trp53*; Muir-Torre syndrome

INTRODUCTION

DNA repair protects the genome from acquiring mutations that may potentially lead to cellular transformation and tumorigenesis. DNA double-strand breaks, the most severe type of DNA lesions, are repaired either by non-homologous end joining or by homologous recombination pathways (1). In homologous recombination, genetic information from a homologous region of a sister chromatid is used as a template to faithfully restore the damaged DNA. Rad51 is a key protein in the homologous recombination pathway, mediating strand invasion and exchange between a free DNA end proximal to a damaged site and a homologous double-stranded DNA (2). Mammalian cells possess an elaborate molecular machinery to ensure a timely and precise loading of Rad51 at sites of DNA damage. This machinery includes five members of the RecA/Rad51 family (Rad51b, Rad51c, Rad51d, Xrcc2, and Xrcc3) that show 20−30% sequence identity to Rad51 (3). These *Rad51* paralogs interact with each other and

*Corresponding author: Mailing address: Building 560, Room 32−31C, 1050 Boyles Street, NCI-Frederick, Frederick, MD 21702, USA. Phone: (301) 846−5140 Fax: (301) 846−7017 Email: sharans@mail.nih.gov.

can be purified as two protein complexes (4,5). One of these complexes includes Rad51b, Rad51c, Rad51d, and Xrcc2 (BCDX2 complex), and the other contains Rad51c and Xrcc3 (CX3 complex). Functional analysis of DNA repair proficiency of double mutants in chicken DT40 cells suggests that these two protein complexes have distinct functions as *Xrcc3* and *Rad51d* double-mutant cells display an additive effect on sensitivity to cisplatin compared with single mutants (6). Each paralog within the BCDX2 complex also appears to contribute differently to the common function based on differential sensitivity to DNA-damaging agents. Rad51c is part of both of these complexes and is thought to play a central role in these associations. Functional analysis has shown that all these genes specifically affect the homologous recombination pathway and suppress recruitment of Rad51 to the site of DNA damage (6,7). Cell lines lacking any of these genes are sensitive to DNA crosslinking agents and are genomically unstable and accumulate chromosomal rearrangements (6,8). In addition to these five paralogs, another member of this family, DMC1, shows 50% sequence identity to Rad51. It is a structural and functional homolog of Rad51 that functions specifically in meiotic recombination (9).

Although a link between *Rad51* family members and cancer is expected, results implicating these genes in cancer thus far have been circumstantial (see ref. 10 for review and references). Overexpression of a dominant-negative form of Rad51 in CHO cells increased tumorigenesis when these cells were transplanted into nude mice. Downregulation of RAD51 was found in patients with multiple myeloma. The product of a balanced translocation between RAD51B (RAD51L1) and a high mobility group protein HMGA2, with subsequent loss of the second RAD51B allele has been implicated in uterine leiomyomas. RAD51D was found to play an important role in telomere maintenance and its E233G variant may be a low-penetrance allele in high-risk breast cancer families without mutations in BRCA1 and BRCA2. A marginal increase in risk ratio has also been found for several XRCC2 and XRCC3 sequence variants in connection with breast and some other types of cancer. RAD51C (RAD51L2) is part of a 17q23 cytoband frequently amplified in sporadic breast cancers (10,11).

Although the above mentioned studies show association of RAD51 family members with cancer, additional verification with larger number of patients is needed (12). In addition, animal studies implicating Rad51 and its paralogs in cancer have been hampered due to early embryonic lethality of mice null for most of these genes (13-18). We have previously reported generation of a conditional allele of *Rad51c* in mouse, where exons 2 and 3 were floxed by insertion of a floxed *PGK-neo* cassette in intron 1 and a single *loxP* site in intron 3 of the *Rad51c* gene (19,20). We used these mice to show the role of Rad51c in meiotic recombination. Here we describe generation of a null allele of *Rad51c* in mice. We show that *Rad51c* is essential for mouse embryonic development and provide evidence that *Rad51c* functions as a tumor suppressor. This study will set a paradigm for the role of other *Rad51* family members in tumorigenesis.

MATERIALS AND METHODS

Construction of the targeting vector

*Kpn*I-*Eco*RI fragment (*13.354 kb)* of the genomic region containing 4 first exons of *Rad51c* was subcloned from the BAC clone RPCI22−514−2C into pBSK(+) plasmid to produce pCSL5 construct. *Thymidine Kinase* (TK) gene (*Not*I-*Bam*HI fragment) under the control of the MC1 promoter was subcloned into pBSK(+) (pSKS11), and subsequently its *NotI-Asp718* fragment was inserted into pCSL5 to produce pCSL5TK construct. *Eco*RV-*Bst*XI fragment (2 kb) from pLMJ237 plasmid containing *loxP*-PGKTn5-*neomycin*-bp(A)-*loxP* was inserted into intron 3 of *Rad51c* in pCSL5TK construct using the lambda-Red recombineering approach (21) and the selection cassette was then deleted by Cre-mediated recombination in bacteria leaving behind a 103 bp-long insert containing a single *loxP* site (pCSL5TKA). In addition, an *Eco*RV-

*Bst*XI fragment (2 kb) from pLTM260 containing an *frt-loxP*-PGK-EM7-*neomycin*-bp(A)-*frt-loxP* cassette was targeted into the first intron of *Rad51c* using lambda-Red recombineering system (pCSL5TKAB8). The resultant targeting vector had a 6.7 kb-homology arm upstream of the first *loxP* site and a 3.8 kb-homology arm downstream of the last *loxP* site.

Targeting of *Rad51c* in ES cells and generation of mutant mice

Targeting vector was linearized with *Sal*I and electroporated into CJ7 ES cells derived from 129S1/SvImJ mouse line. Electroporation and selection were performed with the CJ7 ES cell line as described elsewhere (22). 127 $G418^R$, $FIAU^R$ ES cell clones were screened by Southern analysis of *Eco*RI digested genomic DNA using an external probe (see Fig. 1A) and two of them were found correctly targeted. The presence of the last *loxP* site was confirmed by hybridizing *SpeI*-digested genomic DNA with an internal probe (see Fig. 1A for the restriction site map). One of these ES cell clones was injected into C57BL/6 blastocysts to generate chimeras. One of these chimeras transmitted the targeted allele, $Rad51^{tm1sks}$, denoted as $Rad51c^{neo}$, in the germ line and $Rad51c^{neo/+}$ pups were obtained. To produce a null allele, $Rad51^{tm2sks}$, denoted as $Rad51c^{ko}$, $Rad51c^{neo/+}$ mice were crossed to β-actin-Cre-deleter strain (23). $Rad51c^{ko/+}$ mice have a mixed genetic background inherited from C57BL/6 and 129S1/SvImJ mouse strains, with C3H and CD1 backgrounds from β-actin-Cre strain. The colony was maintained on a mixed genetic background. Littermate controls were used in all studies. Mice were maintained under limited access conditions at the National Cancer Institute (Frederick) and animal care was provided according to the procedures outlined in the Guide for the Care and Use of Laboratory Animals, under an approved animal care and use committee protocol.

Genotyping of *Rad51c* and *Trp53* mutant mice

For genotyping purposes, genomic DNA was extracted from tail biopsies or from frozen tumor tissues according to standard procedures. To genotype for *Rad51c* by Southern blot, 3–5 μg tail DNA was digested overnight with *HpaI*, size-fractionated in a 0.8% agarose gel in TAE buffer for approximately 6 hours to resolve 10 kb and 12 kb bands, and transferred onto a N^+-Hybond nylon membrane (Amersham) by the alkaline transfer method. 531 bp-long *Rad51c* internal probe (Int2) was amplified from pCSL5TK plasmid (F: 5'-TGCCTGAATGTGTCTGCAC-3'; R: 5'-ATAGCAGGCAGCAGCATCT-3') for 40 cycles at 94°C for 40 s, 57°C for 40s, and 72°C for 40 s. The PCR-product was then gel-purified and labeled with ^{32}P-dCTP using the Random Primer Labeling Kit according to manufacturer's instructions. Hybridization was conducted according to standard procedures and band sizes corresponding to *Rad51c* alleles were interpreted as shown in Figure 1C. Genotyping for *Trp53* by Southern blotting was performed as described elsewhere (24).

We also designed a PCR-genotyping strategy to genotype *Rad51c* and *Trp53 mutant mice*. For *Rad51c*, approximately 50 ng of tail or embryo DNA was amplified with the Platinum Taq polymerase (Invitrogen) using a three-primer strategy (F1: 5'-5'ACCGGGCAGTGGTGGCGCACGCCTTTAATCCCAGCACTTG -3'; F2: 5'-CAAAATGCTGGAATAATAGACCTGTGTCATACCCAAAGTG-3'; R1: 5'-GGGTATCCATATCACAGCCACTGTACTCTAGCTCCAGGAG-3') at 94°C for 45 s, 65° C for 42s, and 72°C for 45 s. for 42 cycles (after initial 2 min at 94°C). PCR-products were analyzed by electrophoresis on a 1% agarose gel. The size of PCR products was 414 bp for a null (ko) allele, 524 bp for the wild-type, and 627 bp for the conditional (25) allele (Fig. 1D).

For *Trp53*, tail DNA was amplified with the Platinum Taq polymerase (Invitrogen) using a three-primer strategy (F1: 5'-CCTCAATAAGCTATTCTGCCAGCTG-3' [P53ex5wtF]; F2: 5'-CGTGATATTGCTGAAGAGCTTGGC-3' [P53neoF]; R1: 5'-CTGTCTTCCAGATACTCGGGATAC-3' [P53ex6R]) at 94°C for 30 s, 55°C for 30s, and

72°C for 45 s. for 35 cycles (after initial 2 min at 94°C). PCR-products were analyzed by electrophoresis on a 1% agarose gel. The size of PCR products was 370 bp for a mutant (ko) allele, 320 bp for the wild-type allele.

Generation and aging of mouse cohorts

We studied 5 mouse cohorts as described below. We used *Trp53* heterozygous mice carrying $Trp53^{tm1Brd}$ allele, denoted as $Trp53^{ko}$ (23). To produce the wild-type, $Rad51c^{ko/+}$ and $Trp53^{ko/+}$ as well as double-heterozygous animals with mutant alleles located on different homologous chromosomes (*DH-trans*), we intercrossed $Rad51c^{ko/+}$ and $Trp53^{ko/+}$ mice. *Rad51c* and *Trp53* reside on mouse chromosome 11 only 10 cM apart and are, therefore, linked. To produce mice with mutant alleles on the same homologous chromosome (*DH-cis*), we first mated *DH-trans* mice with the wild-type and selected rare double-heterozygous progeny, which could be obtained only if the two mutant alleles recombined during meiosis. Such mice carrying the two mutant alleles on the same homologous chromosome were then we backcrossed to the wild-type to increase the cohort size. Mice were group-housed with food and water *ad libitum* and were maintained on a 12 hr light/dark cycle. Animals were monitored for 600 days. Sick mice and those with visible tumors were sacrificed and sent for pathological evaluation. One half of each tumor mass identify at necropsy was snap-frozen and stored at −80°C for further LOH analysis.

Immunostaining for MSH2

To test whether a mismatch repair protein Msh2 was specifically lost in preputial and Zymbal's gland tumors, we stained those tissues immunohistochemically. Paraffin slides were first deparaffinized with xylene and then rehydrated through 4 changes of 100% ethanol and one change of 95% ethanol. Endogenous peroxidase was blocked for 15 minutes in 0.6% H_2O_2 in methanol. Heat-induced epitope retrieval (HIER) with 0.01 M citrate buffer (BioGenex Laboratories, San Ramon, CA) was carried out at 100°C for 10 minutes. The slides were then rinsed with PBS for 10 minutes, blocked with goat serum (Vector Labs) for 30 minutes and incubated with primary anti-MSH2 antibody (Abcam, diluted 1:50 in PBS with 0.1% BSA) overnight at 4°C. Slides were then rinsed with PBS and incubated with the biotinylated secondary goat-anti-rabbit antibody (Vector Labs) for 30 minutes, diluted 1:100 in PBS with 10% goat serum, followed by an avidin-biotin peroxidase complex method using the Vector Elite ABC kit (Vector Labs, Burlingame, CA). Reaction was detected using DAB and counterstained with hematoxylin and mounted in Permount™ (Daigger, Vernon Hills, IL).

Generation of *Rad51c*-null MEFs *in vitro* and proliferation test

Due to an early postimplantation lethality of $Rad51c^{ko/ko}$ embryos, no *Rad51c*-null mouse embryonic fibroblast cells (MEFs) could be established by a standard method. Therefore, we generated such cells by infecting MEFs that were homozygous for the conditional *Rad51c* allele ($Rad51c^{neo/neo}$) with adenovirus expressing Cre-recombinase (AD-Cre-GFP, Viral Technology Laboratory, NCI-Frederick). Primary MEFs were isolated from E13.5 F1 embryos obtained from a $Rad51c^{neo/+}$ mother backcrossed on C57BL/6 genetic background for 7 generations and a $Rad51c^{neo/+}$ father backcrossed on 129/SvEv genetic background for 8 generations. Exponentially growing MEFs (P1) were trypsinized and resuspended in a small volume of the culture medium (DMEM supplemented with penicillin and streptomycin and 15% FBS) at 3×10^7 cells/ml. A 100 μl aliquot containing 3×10^6 cells was mixed with 3 μl AD-Cre-GFP suspension (3×10^7 viral particles) to achieve 10 MOI (Multiplicity Of Infection) ratio. The mixture was allowed to stand for 30 minutes at room temperature and then split between two 10 cm tissue culture dishes. Infection efficiency was evaluated the next day by GFP expression. Genotyping for *Rad51c* by Southern blot was used to confirm 100% recombination efficiency. Four days after infection, the cells were collected and seeded at 0.3×10^6 cells per

one 6 cm dish in duplicates for a proliferation assay according to the 3T3 protocol. Cells were collected and counted every 3 days and seeded again at 0.3×10^6 cells per dish for 6 consecutive passages. Average increase in cell number was calculated for each passage and plotted as a cumulative growth.

Isolation of *Rad51c*-null MEFs from embryos

To isolate *Rad51c*-null MEFs, on *Trp53*-null background, we intercrossed a pair of *DH-cis* mice and dissected embryos at E10.5. At that point double-mutant embryos appeared morphologically similar to normal E9.5 embryos. Cells were explanted from embryo carcasses into 10 cm tissue culture dishes by standard techniques and incubated at 3% oxygen concentration to suppress cellular senescence (26). Initially, mutant cells grew poorly and had to be split at a very low dilution ratio for the first 5−7 passages. At approximately P10, the cell lines stabilized and grew at a similar speed as control MEFs (data not shown). Control $Trp53^{ko/ko}$ MEFs were isolated from E9.5 embryos essentially the same way.

Drug sensitivity test

We tested the effect of DNA-damaging compounds on mutant cell proliferation *in vitro*. Two independent cell lines were tested for each genotype: $Rad51c^{ko/ko}$; $Trp53^{ko/ko}$ double-null, $Trp53^{ko/ko}$ single-null control, and the wild type. We seeded 4,000 cells per well in gelatinized 24-well plates in duplicates for each line. Continuous drug treatment was started in 18 h at the following doses: mitomycin C (MMC) at 0, 10, 20, and 30 ng/ml, methylmethane sulfonate (MMS) at 0, 5, 10, and 15 μg/ml. Cells from one plate were trypsinized and counted using a Coulter counter and used as a control for plating efficiency and as a "before treatment" day1 reference. Two days later (3^{rd} day after seeding) the remaining cells were counted the same way. Day1 reference numbers were subtracted from day 3 cell numbers to evaluate growth of each cell line. The resulting cell counts were expressed as percentages from the untreated wells.

Rad51 foci formation assay

We plated 40,000 cells per well in gelatinized Tissue Culture Treated Glass slides (Falcon). We irradiated slides 48 h later with 10 Gy. Six hours after irradiation, we fixed the cells with 4% paraformaldehyde for 5 min, washed them twice with PBS and permeabilized in PBS-buffered 0.1% Triton X-100 for 10 min. After two additional washes with PBS, we blocked cells in a blocking solution (1% BSA, 0.05% Triton X-100, 10% donkey serum in PBS). We performed antibody staining and imaging as described previously (27). 10−15 images with a total of at least 50 cells have been scored for Rad51 and γH2AX foci.

Chromosomal aberration test

We treated MEFs with colcemid (Invitrogen) for 1.5 h to arrest them at metaphase. The cells were then trypsinized, washed and resuspended in hypotonic solution at 37 °C (0.075M KCl) for 15 min and fixed in a methanol–acetic acid mixture (3:1 vol/vol). We stained air-dried preparations in Giemsa solution (10% Sorensen's buffer and 2% Giemsa, J.T. Baker). 200 well spread metaphases containing at least 40 chromosomes from each genotype were examined blindly for structural aberrations.

Statistical analysis

Animal survival and tumor latency data were processed using the survival / reliability function and *P*-values were estimated using the Wilcoxon test using the JMP 5.0.1a statistical software package. Numbers of Rad51 and γH2AX foci in MEFs were evaluated using basic statistics functions in JMP. Because γH2AX foci showed a bimodal distribution, we separated the cells into groups A and B depending on the number of observed foci and evaluated them separately.

Deviation of genotype segregation from the Mendelian ratio at various developmental stages was calculated using chi test function in MS Excel (Supplementary Table 1).

RESULTS

Gene targeting and embryonic lethality of *Rad51c*$^{ko/ko}$ mice

To generate a constitutive knockout allele, we crossed the mice carrying the floxed allele of *Rad51c* (*Rad51*^{tm1sks}, denoted hereafter as *Rad51c*^{neo}) that retains the neomycin resistance gene (25) to mice expressing *Cre* recombinase under the control of the human ß-actin promoter (28). The resulting allele, *Rad51*^{tm2sks} denoted hereafter as *Rad51c*^{ko}, lacked exons 2 and 3 that code for a 142-amino acid region, including a linker region and an ATPase motif called Walker A (Fig. 1A, B). Walker A motif is indispensable for the function of Rad51 family proteins (19,29). No mature Rad51c protein could be detected from this allele as has been shown previously (19,29). We obtained *Rad51c* heterozygous (*Rad51c*$^{ko/+}$) mice that were viable and fertile and indistinguishable from their wild-type littermates.

When *Rad51c*$^{ko/+}$ mice were intercrossed, we did not obtain homozygous mutant (*Rad51c*$^{ko/ko}$) offspring (Supplementary Table 1), which suggested that these mice die during embryogenesis. In addition, the number of *Rad51c*$^{ko/+}$ newborn mice relative to the wild-type (239 and 156, respectively) deviated from the Mendelian 2:1 ratio and indicated that some *Rad51c*$^{ko/+}$ mice die during gestation. To determine the cause and time of lethality, we dissected embryos from a *Rad51c*$^{ko/+}$ intercross at various gestational stages between E5.5 – E10.5. At all stages with the exception of E8.5, approximately 25% of all embryos had an abnormal phenotype (Fig. 2 and Supplementary Table 1). Genotyping of E7.5 and E8.5 embryos confirmed that phenotypically abnormal embryos were indeed *Rad51c*$^{ko/ko}$. At E8.5, 39% of all embryos (n=126) were phenotypically abnormal. We found that 2 out of 18 phenotypically abnormal embryos at this stage were heterozygous for *Rad51c* while the remaining 16 *Rad51c*$^{ko/+}$ embryos were indistinguishable from the wild-type littermates (Supplementary Table 1). This partial embryonic lethality of heterozygous mice may account for a sub-Mendelian ratio of *Rad51c*$^{ko/+}$ relative to wild-type newborn mice. Although its exact cause is currently unknown, we speculate that this may be due to mixed genetic background (see Discussion section).

At E5.5 the mutant embryos lacked the proamniotic cavity and exhibited a slight delay in development (Fig. 2A, top). At E6.5 – E7.5 the delay in development of the embryo proper further increased while extraembryonic tissues continued to grow comparable to control littermates (Fig.2A, bottom and Fig. 2B top). The degeneration processes became evident after E8.5 (Fig. 2B, bottom). At this stage *Rad51c*$^{ko/ko}$ embryos usually formed neural folds but looked severely abnormal and underwent resorption shortly thereafter. Histological evaluation of the *Rad51c*$^{ko/ko}$ embryos did not reveal failure of any specific tissue type, but rather an overall growth defect of embryonic tissues. BrdU labeling of proliferating cells and TUNEL staining of cells with fragmented genomic DNA indicated that a marked increase in apoptosis occurred in the *Rad51c*$^{ko/ko}$ embryos at the E8.5 developmental stage (Fig. 2C).

Genetic interaction between *Rad51c* and *Trp53*

Defects in DNA repair often lead to apoptosis, which can be ameliorated on a *Trp53*-deficient genetic background (14,17). To examine whether the lethality of *Rad51c*-null embryos can be rescued by the lack of *Trp53* and to have a better understanding of the cause of embryonic lethality, we crossed *Rad51c*$^{ko/+}$ mice to *Trp53* heterozygous mice carrying *Trp53*^{tm1Brd} allele, denoted hereafter as *Trp53*^{ko} (24). We generated mice in which mutant alleles of these two genes (*Rad51c*$^{ko/+}$*;Trp53*$^{ko/+}$) resided in the same chromosome (double heterozygous-*cis, DH-cis*, Fig. 3A) and, thus, were inherited as a single genetic locus. No double-homozygous mutant

(*Rad51c*$^{ko/ko}$;*Trp53*$^{ko/ko}$) offspring was obtained from *DH-cis* intercrosses. However, at E10.5, 25% of the embryos were confirmed to be *Rad51c*$^{ko/ko}$;*Trp53*$^{ko/ko}$. These mutant embryos are developmentally similar to an E10.5 embryo with a normal looking heart but the embryos are smaller in size (Fig. 2D). In addition, these embryos have truncated caudal region and unclosed head folds. The fact that *Rad51c*$^{ko/ko}$ embryos were severely degenerated after E8.5, and double-null embryos apparently progressed until E10.5 stage (Fig. 2B bottom and Fig. 2D), implied that embryonic development of *Rad51c*$^{ko/ko}$ mice could be partially rescued by the loss of *Trp53*. In addition, cells from *Rad51c*$^{ko/ko}$ embryos failed to proliferate *in vitro* but MEF lines from *Rad51c*$^{ko/ko}$;*Trp53*$^{ko/ko}$ could be successfully generated (data not shown). These results suggest that lethality of *Rad51c*$^{ko/ko}$ embryos is due the apoptotic response to a DNA repair defect.

Rad51c has a gender-specific effect on tumor latency

To date there is no definitive evidence that RAD51 or any of its paralogs function as a tumor suppressor (12). It is likely that loss of any of these essential proteins triggers a severe proliferation defect, cell-cycle arrest and/or apoptosis (30). To examine the role of *Rad51c* in tumorigenesis, we aged *Rad51c*$^{ko/+}$ and wild-type littermates. In addition, to provide a cellular environment that lacks normal cell cycle checkpoints and allows proliferation of *Rad51c*$^{ko/ko}$ cells, we also monitored the tumor predisposition of *Rad51c*$^{ko/+}$ mice on a *Trp53*$^{ko/+}$ genetic background. We monitored the *DH-cis* mice (Fig. 3A), in which we expected a single loss-of-heterozygosity event to result in a simultaneous loss of the wild-type alleles of both *Rad51c* and *Trp53*. As a control, we used mice in which the mutant alleles of the two genes are on different homologues (double heterozygous-*trans, DH-trans* Fig. 3A). We also aged *Trp53*$^{ko/+}$ as a second control group, to examine the effect of *Trp53* loss alone.

We found no significant difference between the tumor latency of *Rad51c*$^{ko/+}$ and wild-type control littermates suggesting that heterozygosity for *Rad51c* alone does not increase the tumor susceptibility in mice (Table 1). However, among females, *DH-cis* mice developed tumors with a significantly shorter latency (369 days) than any other group including *DH-trans* (461 days) and *Trp53*$^{ko/+}$ (475 days) mice (Fig. 3B and Table 1). In contrast, *DH-cis* males did not show a significant difference in tumor-free survival from other groups with a mutation in *Trp53*. Interestingly, *DH-trans* and *Trp53*$^{ko/+}$ males developed tumors earlier than females of the same genotype, while the correlation was reversed for *DH-cis* mice. We conclude that, first, the tumor latency of *DH-trans* is similar to that of *Trp53*$^{ko/+}$ mice and, second, it is functionally important whether mutations of *Rad51c* and *Trp53* are located on the same or on different homologous chromosomes.

Tumor Spectrum of *DH-cis* mice is different from *DH-trans* and *Trp53*$^{ko/+}$

In addition to tumor latency, we also found significant differences in tumor spectrum between mice of different genotypes and genders. Consistent with previous reports (31,32), the most common types of neoplasms in *Trp53*$^{ko/+}$ females were osteosarcomas, mammary adenocarcinomas and lymphomas (Table 2 and Supplementary Table 2). *Trp53*$^{ko/+}$ males, on the other hand, usually succumbed to muscle sarcomas, lung cancer, and hematopoietic malignancies. As with the tumor latency, the tumor spectrum of *DH-trans* mice was also remarkably similar to *Trp53*$^{ko/+}$ mice. In contrast, *DH-cis* mice developed fewer tumors characteristic for *Trp53*-deficient mice, but revealed a greatly increased incidence of unique tumor types such as tumors of specialized sebaceous glands and tissues in the muzzle area (nasal and periocular region, Table 2).

Preputial gland carcinoma was the most frequent type of sebaceous tumors in *DH-cis* males found in 10 out of 24 animals (42%). Four of these ten animals additionally developed Zymbal's gland carcinomas and a fifth had a Harderian gland adenoma, all being glands secreting lipids.

Another animal had a Zymbal's gland carcinoma only. We also found preputial gland carcinoma in one *DH-trans* male and a Zymbal's gland carcinoma in two *DH-trans* females. In all the mice we monitored, there was only one case of Zymbal's gland carcinoma in a mouse that did not have a *Rad51c* mutation (in $Trp53^{ko/+}$ group).

Analysis of the tumor spectrum can also explain the differences in the tumor-free survival time between genders and different genotypes. Those neoplasms that appeared to be the probable cause of death or were a primary indication for clinical sacrifice in *DH-cis* females included mammary gland carcinomas and carcinomas of the skin and nasal malignancies, and were the major contributors to their shorter survival (average tumor latencies of 371, 323, and 331 days, respectively). A shift from aggressive *Trp53*-characteristic tumor types to preputial and Zymbal's gland carcinomas and hematopoietic neoplasms in *DH-cis* males (463, 446, and 398 days, respectively), was probably responsible for a longer survival in this group. In $Trp53^{ko/+}$ and *DH-trans* males, muscle sarcomas were a single tumor type that had a decisive impact on the survival time (average latency for 11 muscle sarcomas in $Trp53^{ko/+}$ males was 308 days, and 255 days for 13 muscle sarcomas in *DH-trans* males).

LOH in tumors

In tumor cells, loss of the wild-type allele at a heterozygous locus for a tumor suppressor gene, like *Trp53*, is considered to be one of the primary mechanisms of tumor progression (33,34). If LOH was indeed the leading mechanism of tumor initiation in this study, the tumor tissues from *DH-trans* mice would be genotypically identical to tumors from *Trp53* heterozygous mice. In contrast, *DH-cis* mice should reveal the loss of both *Rad51c* and *Trp53* genes. To test this, we genotyped the tumor samples collected from these animals by Southern blot analysis (Fig. 3D). As expected, all 24 tumor samples from $Trp53^{ko/+}$ mice showed the loss of the wild-type allele. Similarly, with the exception of one sample, all tumors from *DH-trans* mice (n=33) lost the wild type copy of *Trp53* and the mutant allele of *Rad51c*. Out of 32 tumors from *DH-cis* mice, 29 revealed the loss of the wild-type allele for both *Trp53* and *Rad51c*. One *DH-cis* tumor sample lost a wild-type copy of *Trp53* without losing *Rad51c* (Fig. 3D). The remaining two tumor samples did not reveal LOH for any of the two genes. Tumors from $Rad51c^{ko/+}$ animals (n=19) did not reveal LOH for *Rad51c*, except in one case. To test the possibility that *Rad51c* might be silenced epigenetically in these tumors, we examined its expression by RT-PCR. We found *Rad51c* to be expressed in all tumors tested (data not shown). Considering the fact that both the tumor latency and the spectrum in $Rad51c^{ko/+}$ mice were similar to the wild type mice, we concluded that *Rad51c* heterozygosity alone does not contribute to tumorigenesis. In contrast, when a loss of *Rad51c* was accompanied by a simultaneous loss of *Trp53*, mice developed tumors in specialized sebaceous glands.

Rad51c and sebaceous tumors

As described above, *DH-cis* males were highly prone to tumors of specialized sebaceous glands, particularly preputial and Zymbal's glands (Supplementary Fig. 1A and B). Sebaceous tumors from human patients often have a dysfunctional mismatch DNA repair pathway and are usually marked by downregulation of Msh2 protein expression and microsatellite instability (35). Therefore, we tested 12 sebaceous tumors for 5 microsatellite markers (D1Mit62, D15Mit93, D17Mit72, uPAR, and pro-1) and found no evidence of microsatellite instability (data not shown). We also tested three of these tumors for expression of Msh2 on paraffin sections. In all three cases the bulk of the tumor tissues stained strongly positive for this marker (Supplementary Fig. 2D), which may indicate either an upregulation of this protein in the tumors or a neoplastic transformation of already existing Msh2-positive cells normally residing at the base of each follicle (Supplementary Fig. 2B). From these results we concluded that a defect in mismatch repair was not responsible for sebaceous tumors in *DH-cis* mice.

In vitro phenotype of *Rad51c*-deficient cells explains its function as a tumor suppressor

How does loss of *Rad51c* promote tumorigenesis? To answer this question, we investigated the effect of *Rad51c* loss at the cellular level. Because of the early embryonic lethality, isolation of MEFs from *Rad51c*$^{ko/ko}$ embryos was not possible. Therefore, in order to generate *Rad51c*$^{ko/ko}$ *MEFs*, we infected *Rad51c*$^{neo/neo}$ MEFs expressing a conditional allele of *Rad51c* with adenovirus expressing *Cre* recombinase. The resultant *Rad51c*$^{ko/ko}$ MEFs, however, suffered a severe growth arrest after 2−3 passages (Fig. 4A), supporting the conclusion that *Rad51c* is essential for cell proliferation.

As reported previously (19), we obtained two independent *Rad51c-null* MEF lines from E10.5 *Rad51c*$^{ko/ko}$*; Trp53*$^{ko/ko}$ embryos (data not shown). We tested the ability of *Rad51c*-deficient cells to repair the DNA damage by challenging them with DNA-crosslinking agent mitomycin C (MMC) or DNA alkylating compound methylmethane sulfonate (MMS). We found the *Rad51c*$^{ko/ko}$*; Trp53*$^{ko/ko}$ MEFs to be 2−3 times more sensitive to both agents compared with *Trp53*$^{ko/ko}$ or wild-type MEFs (Fig. 4B). This observation is consistent with previously published data on *Rad51c*-deficient hamster CL-V4B and chicken DT40 cell lines (6,36), although the degree of drug sensitivity of the MEFs was lower than that of hamster and chicken counterparts.

Rad51c-deficient mammalian cells have been previously reported to have attenuated Rad51 foci after ionizing irradiation, thus, implicating Rad51c in recruitment of Rad51 to sites of DNA damage and repair (6,7). While we observed an average of 26 foci in 62% of wild-type cells (N=62) and 28 foci in 86% of *Trp53*$^{ko/ko}$ MEFs (N=55) 6 hrs after 10 Gy of γ-irradiation, no Rad51 foci could be found in *Rad51c*$^{ko/ko}$*; Trp53*$^{ko/ko}$ MEFs (Fig. 4C and Supplementary Table 3). In addition, unirradiated *Rad51c*$^{ko/ko}$*; Trp53*$^{ko/ko}$ MEFs revealed more γH2AX foci-positive cells (78% vs. 22−39% in controls) than the control MEFs suggesting the presence of abnormally large amount of damaged DNA even without exposure to any DNA damaging agent.

Increased DNA damage and dysfunctional DNA repair leads to genomic instability. We determined the frequency of various chromosomal aberrations in mutant and control MEFs with or without treatment with a low dose of MMC (10 ng/ml) corresponding to a LD_{10} for wild-type MEFs (Fig. 4B and C). While an average of 106 chromosomal aberrations per 100 cells was observed in untreated *Trp53*$^{ko/ko}$ MEFs, their number increased to 150 in *Rad51c*$^{ko/ko}$*; Trp53*$^{ko/ko}$ MEFs, suggesting that there is a constant level of DNA damage persisting in double-mutant cells even without a genotoxic treatment. This is consistent with the increased proportion of γH2AX-positive cells in unirradiated culture as described above. After treatment, the number of chromosomal aberrations in *Rad51c*$^{ko/ko}$*; Trp53*$^{ko/ko}$ MEFs increased to 496 per 100 cells compared with only 170 aberrations per 100 cells in *Trp53*$^{ko/ko}$ MEFs. The most frequent types of aberrations were radial structures, chromosomal fragments, chromatid gaps and breaks, which is consistent with the effect of MMC. It is worth noting that the number of chromosomal aberrations in primary wild-type and *Rad51c*$^{ko/+}$ MEFs was significantly lower compared with *Rad51c*$^{ko/ko}$*; Trp53*$^{ko/ko}$ and *Trp53*$^{ko/ko}$ MEFs . This may reflect disruption of some cellular pathways involved in chromosomal stability during establishing the cell lines in culture. Taken together, tumors arising from *DH-cis* mice, which became functionally null for both *Rad51c* and *Trp53* in most cases, are predicted to be deficient in DNA repair and genetically unstable and, thus, different from *DH-trans* tumors. This may have had a significant influence on the tissue specificity of tumors that developed in these mice as it is known for many other DNA repair genes.

DISCUSSION

Functional analysis of Rad51 paralogs

Here we describe generation of a null allele of *Rad51c* and show that *Rad51c* is essential for viability in mice. Like *Rad51c*, loss of other Rad51 paralogs in mice also results in embryonic lethality. *Rad51b-null* embryos almost completely disappear as early as E7.5 and have the most severe phenotype among all paralogs (17). *Rad51d*-deficient embryos die between E9.0 and E10.0 (16). *Xrcc2*-mutant embryos develop normally through E8.5 (15). However, approximately 75% of the mutant embryos die between E10.5 – E12.5. Some even survive to birth but die within 20 minutes due to underinflated lungs. The phenotype associated with loss of *Xrcc3* in mice is not known. Interestingly, the severity of the embryonic phenotype of *Rad51b*, *Rad51c*, and *Rad51d* directly correlates with respective cellular phenotypes in DT40 cells in terms of sensitivity to stalled replication forks induced by a topoisomerase I inhibitor, camptothecin, rather than relative sensitivity to DNA interstrand crosslinks induced by cisplatin (6). In spite of their overlapping functions, each paralog results in a distinct phenotype. This suggests that these paralogs may have other unique functions. Indeed, *Rad51d* is shown to be essential for telomere stability (37). A role in meiotic recombination and resolution of Holliday junctions (HJs) has been demonstrated for *Rad51c* and *Xrcc3* and this function is evolutionary conserved through *Arabidopsis thaliana* (19,38-40).

Rad51c is a tumor suppressor

Rad51c is evidently essential for DNA repair. Therefore, we expected an increase in tumor predisposition in $Rad51c^{ko/+}$ mice due to genomic instability in cells undergoing LOH at *Rad51c* locus. Failure to observe LOH in this group can be attributed to the fact that loss of the *Rad51c* function may be too detrimental for a cell, thus, causing its elimination prior to the neoplastic transformation. The fact that, during the 600-day period that we monitored the mice for tumors, the tumor latency, spectrum, and frequency did not significantly differ between $Rad51c^{ko/+}$ and wild-type mice, supports our conclusion that heterozygosity for *Rad51c* alone does not predispose mice to cancer.

Because loss of *Trp53* function can delay the onset of apoptosis in cells experiencing a severe proliferation defect due to *Rad51c* deficiency, we examined the tumor susceptibility of $Rad51c^{ko/+}$ mice on a $Trp53^{ko/+}$ genetic background. We monitored two classes (*DH-trans* and *DH-cis*) of genotypically identical $(Rad51c^{ko/+};Trp53^{ko/+})$ mice. It was intriguing to find that these two classes produced distinctly different tumor types. LOH analysis revealed that most of the tumors from *DH-cis* mice lost the wild-type alleles of both *Trp53* and *Rad51c* while *DH-trans* mice lost the wild-type allele of *Trp53* along with the mutant allele of *Rad51c* but retained its wild-type allele. This result strongly suggests that *Rad51c* plays an important role in tumor formation, albeit *Trp53*-dependent. Such dependence on *Trp53* loss has been reported for many other tumor suppressor genes (e.g. *Brca1, Brca2, Fbxw7/Cdc4*) (41-44). Although tumor latency in *DH-cis* mice is primarily determined by the LOH at the *Trp53* locus, additional loss of *Rad51c* essentially overrides the tissue-specific effect of *Trp53* mutation and promotes a shift from sarcomas (mesodermal origin) to malignancies of skin and adrexia (epidermal origin) especially those of specialized sebaceous glands and other glandular and neuroepithelial tissues such as those in the nasal and periocular area. Therefore, we conclude that *Rad51c* should be considered a *Trp53*-dependent tumor suppressor. However, we cannot rule out the possibility that there are strain-specific modifiers linked to the originating alleles of the *Trp53* and *Rad51c* knockouts that, when combined, alter the tumor spectrum in *DH-cis* and *DH-trans* mice.

Why are *Rad51c*-tumors tissue-specific?

Our findings raise two important questions: how does loss of *Rad51c* give rise to malignancies that are tissue specific in spite of its role in DNA repair in every cell, and how does addition of *Rad51c*-deficiency prevent development of *Trp53*-characteristic tumors in compound heterozygotes? In regards to the first question, examples of tissue-specific tumors caused by defects in genes that are essential for every cell type are well known. Genes like *BRCA1* and *BRCA2* are involved in DNA double-strand break repair but are predominantly associated with breast and ovarian cancer (45). Similarly, *MLH1*, *PMS2*, and *MSH2* are important mismatch repair genes but their mutations lead to colon cancer (46,47). The cause of the tissue-specific phenotype for these genes remains to be understood. It is possible that some downstream genes mutated in the absence of such DNA repair genes are responsible for the tissue-specific phenotype. Alternatively, these DNA repair genes may be directly involved in differentiation of certain tissues so that their dysfunction leads to a tissue-specific neoplastic transformation.

How *Rad51c*-deficiency can prevent development of *Trp53*-characteristic tumors such as to osteosarcomas and muscle sarcomas is unclear (Table 2). One possibility is that LOH for *Rad51c* may interfere with survival, differentiation, or neoplastic transformation of the cells that give rise to these tumors. This is supported by the observation that one of the six osteosarcoma samples from *DH-cis* females shows LOH only for *Trp53* and not for *Rad51c* (Fig. 3D, see T11a). Interestingly, a myoepithelioma in the salivary gland of the same animal exhibits loss of wild-type alleles of both *Rad51*c and *Trp53*. Identification of the cell types that give rise to osteosarcomas and muscle sarcoma and the role of *Rad51c* in these cells will help understand the cause of reduction of these tumor types in *DH-cis* mice.

Tumors of specialized sebaceous glands in *DH-cis* mice

The high frequency of tumors in specialized sebaceous glands in *DH-cis* mice is unique and unexpected. Preputial gland tumors are rare in rodents (2.9% frequency reported for rats and even less for mice) (48) and have been reported to develop in only a few mouse models (49), (50). In humans, 75% of sebaceous tumors arise in the periocular region, often from a specialized sebaceous gland of the eyelid, the meibomian gland (similar to *DH-cis* mouse tumor shown in Supplementary Fig. 1E) (51,52). This type of malignancy is rare but aggressive and represents 1−5.5% of eyelid malignancies (52). A small portion of sebaceous tumors is associated with Muir-Torre syndrome (53). The etiology of sebaceous cancers is unclear, but most MTS patients were found deficient in the mismatch repair pathway, primarily due to loss of MSH2 protein (54). In tumors from *DH-cis* mice we did not find any loss or downregulation of Msh2 or microsatellite instability, suggesting that the mismatch repair mechanism is not involved.

Partial lethality of *Rad51c*$^{ko/+}$: haploinsufficiency or a modifier effect?

Some *Rad51c*$^{ko/+}$ embryos also had an abnormal phenotype and the ratio of viable *Rad51c*$^{ko/+}$ mice was sub-Mendelian relative to the wild-type. Haploinsufficiency is unlikely to be the cause of partial *Rad51c*$^{ko/+}$ lethality because no lethality was observed previously for *Rad51c*$^{ko/neo}$ mice expressing only 15−40% of the normal protein level (19,38-40). We speculate that the presence of genetic modifiers may play a role. It is possible that one or several alleles co-segregating with the mutant allele of *Rad51c* may have overtly affected survival.

In conclusion, our results suggest that *Rad51c* functions as a tumor suppressor in mice. This is the first demonstration of a role in tumorigenesis for any *Rad51* family member in mice. Similar studies may reveal unexpected tissue-specific effects for other Rad51 family members. Our future studies will be focused on examining the role of *Rad51c* in human tumors and on understanding the tissue-specific functions of *Rad51c* in epithelial tissues.

Supplementary Material

Refer to Web version on PubMed Central for supplementary material.

Acknowledgements

We thank J. Acharya, K. Biswas, S. Chang, I. Daar, S. Philip, K.Reilly, E. Sterneck and L. Tessarollo for helpful discussions and critical review of the manuscript. We also thank B. Martin, E. Southon, S. Reid, D. Butcher, and S. Burkett for technical assistance; J. Wada for illustrations; M. Lewandoski for providing the β-actin-Cre mouse strain. The research was sponsored by the Center for Cancer Research, National Cancer Institute, US National Institutes of Health.

REFERENCES

1. Shrivastav M, De Haro LP, Nickoloff JA. Regulation of DNA double-strand break repair pathway choice. Cell Res 2008;18:134–47. [PubMed: 18157161]
2. Bianco PR, Tracy RB, Kowalczykowski SC. DNA strand exchange proteins: a biochemical and physical comparison. Front Biosci 1998;3:D570–603. [PubMed: 9632377]
3. Kawabata M, Kawabata T, Nishibori M. Role of recA/RAD51 family proteins in mammals. Acta Med Okayama 2005;59:1–9. [PubMed: 15902993]
4. Masson JY, Tarsounas MC, Stasiak AZ, et al. Identification and purification of two distinct complexes containing the five RAD51 paralogs. Genes Dev 2001;15:3296–307. [PubMed: 11751635]
5. Masson JY, Stasiak AZ, Stasiak A, Benson FE, West SC. Complex formation by the human RAD51C and XRCC3 recombination repair proteins. Proc Natl Acad Sci U S A 2001;98:8440–6. [PubMed: 11459987]
6. Yonetani Y, Hochegger H, Sonoda E, et al. Differential and collaborative actions of Rad51 paralog proteins in cellular response to DNA damage. Nucleic Acids Res 2005;33:4544–52. [PubMed: 16093548]
7. van Veelen LR, Essers J, van de Rakt MW, et al. Ionizing radiation-induced foci formation of mammalian Rad51 and Rad54 depends on the Rad51 paralogs, but not on Rad52. Mutat Res 2005;574:34–49. [PubMed: 15914205]
8. Takata M, Sasaki MS, Tachiiri S, et al. Chromosome instability and defective recombinational repair in knockout mutants of the five Rad51 paralogs. Mol Cell Biol 2001;21:2858–66. [PubMed: 11283264]
9. Pittman DL, Cobb J, Schimenti KJ, et al. Meiotic prophase arrest with failure of chromosome synapsis in mice deficient for Dmc1, a germline-specific RecA homolog. Mol Cell 1998;1:697–705. [PubMed: 9660953]
10. Thacker J. The RAD51 gene family, genetic instability and cancer. Cancer Lett 2005;219:125–35. [PubMed: 15723711]
11. Bärlund M, Tirkkonen M, Forozan F, et al. Increased copy number at 17q22-q24 by CGH in breast cancer is due to high-level amplification of two separate regions. Genes Chromosomes Cancer 1997;20:372–6. [PubMed: 9408753]
12. Parssinen J, Kuukasjarvi T, Karhu R, Kallioniemi A. High-level amplification at 17q23 leads to coordinated overexpression of multiple adjacent genes in breast cancer. Br J Cancer 2007;96:1258–64. [PubMed: 17353917]
13. Lim DS, Hasty P. A mutation in mouse rad51 results in an early embryonic lethal that is suppressed by a mutation in p53. Mol Cell Biol 1996;16:7133–43. [PubMed: 8943369]
14. Adam J, Deans B, Thacker J. A role for Xrcc2 in the early stages of mouse development. DNA Repair (Amst) 2007;6:224–34. [PubMed: 17116431]
15. Deans B, Griffin CS, Maconochie M, Thacker J. Xrcc2 is required for genetic stability, embryonic neurogenesis and viability in mice. Embo J 2000;19:6675–85. [PubMed: 11118202]
16. Pittman DL, Schimenti JC. Midgestation lethality in mice deficient for the RecA-related gene, Rad51d/Rad51l3. Genesis 2000;26:167–73. [PubMed: 10705376]
17. Shu Z, Smith S, Wang L, Rice MC, Kmiec EB. Disruption of muREC2/RAD51L1 in mice results in early embryonic lethality which can Be partially rescued in a p53(−/−) background. Mol Cell Biol 1999;19:8686–93. [PubMed: 10567591]

18. Tsuzuki T, Fujii Y, Sakumi K, et al. Targeted disruption of the Rad51 gene leads to lethality in embryonic mice. Proc Natl Acad Sci U S A 1996;93:6236–40. [PubMed: 8692798]
19. Kuznetsov S, Pellegrini M, Shuda K, et al. RAD51C deficiency in mice results in early prophase I arrest in males and sister chromatid separation at metaphase II in females. J. Cell Biol 2007;176:581–92. [PubMed: 17312021]
20. Leasure CS, Chandler J, Gilbert DJ, et al. Sequence, chromosomal location and expression analysis of the murine homologue of human RAD51L2/RAD51C. Gene 2001;271:59–67. [PubMed: 11410366]
21. Liu P, Jenkins NA, Copeland NG. A Highly Efficient Recombineering-Based Method for Generating Conditional Knockout Mutations. Genome Res 2003;1:476–84. [PubMed: 12618378]
22. Tessarollo L. Manipulating mouse embryonic stem cells. Methods Mol Biol 2001;158:47–63. [PubMed: 11236671]
23. Meyers EN, Lewandoski M, Martin GR. An Fgf8 mutant allelic series generated by Cre- and Flp-mediated recombination. Nat Genet 1998;18:136–41. [PubMed: 9462741]
24. Donehower LA, Harvey M, Slagle BL, et al. Mice deficient for p53 are developmentally normal but susceptible to spontaneous tumours. Nature 1992;356:215–21. [PubMed: 1552940]
25. Hughes-Davies L, Huntsman D, Ruas M, et al. EMSY links the BRCA2 pathway to sporadic breast and ovarian cancer. Cell 2003;115:523–35. [PubMed: 14651845]
26. Parrinello S, Samper E, Krtolica A, et al. Oxygen sensitivity severely limits the replicative lifespan of murine fibroblasts. Nat Cell Biol 2003;5:741–7. [PubMed: 12855956]
27. Kuznetsov SG, Liu P, Sharan SK. Mouse embryonic stem cell-based functional assay to evaluate mutations in BRCA2. Nat Med 2008;14:875–81. [PubMed: 18607349]
28. Lewandoski M, Meyers EN, Martin GR. Analysis of Fgf8 gene function in vertebrate development. Cold Spring Harb Symp Quant Biol 1997;62:159–68. [PubMed: 9598348]
29. French CA, Tambini CE, Thacker J. Identification of functional domains in the RAD51L2 (RAD51C) protein and its requirement for gene conversion. J Biol Chem 2003;278:45445–50. [PubMed: 12966089]
30. Brown EJ. Analysis of cell cycle progression and genomic integrity in early lethal knockouts. Methods Mol Biol 2004;280:201–12. [PubMed: 15187255]
31. Kuperwasser C, Hurlbut GD, Kittrell FS, et al. Development of spontaneous mammary tumors in BALB/c p53 heterozygous mice. A model for Li-Fraumeni syndrome. Am J Pathol 2000;157:2151–9. [PubMed: 11106587]
32. Hwang SJ, Lozano G, Amos CI, Strong LC. Germline p53 mutations in a cohort with childhood sarcoma: sex differences in cancer risk. Am J Hum Genet 2003;72:975–83. [PubMed: 12610779]
33. Tamura G. Alterations of tumor suppressor and tumor-related genes in the development and progression of gastric cancer. World J Gastroenterol 2006;12:192–8. [PubMed: 16482617]
34. Harvey M, McArthur MJ, Montgomery CA, et al. Spontaneous and carcinogen-induced tumorigenesis in p53-deficient mice. Nat Genet 1993;5:225–9. [PubMed: 8275085]
35. Entius MM, Keller JJ, Drillenburg P, et al. Microsatellite instability and expression of hMLH-1 and hMSH-2 in sebaceous gland carcinomas as markers for Muir-Torre syndrome. Clin Cancer Res 2000;6:1784–9. [PubMed: 10815898]
36. Wojcik A, Stoilov L, Szumiel I, Legerski R, Obe G. Rad51C-deficient CL-V4B cells exhibit normal levels of mitomycin C-induced SCEs but reduced levels of UVC-induced SCEs. Biochem Biophys Res Commun 2005;326:805–10. [PubMed: 15607741]
37. Tarsounas M, Munoz P, Claas A, et al. Telomere maintenance requires the RAD51D recombination/repair protein. Cell 2004;117:337–47. [PubMed: 15109494]
38. Bleuyard JY, Gallego ME, Savigny F, White CI. Differing requirements for the Arabidopsis Rad51 paralogs in meiosis and DNA repair. Plant J 2005;41:533–45. [PubMed: 15686518]
39. Liu Y, Masson JY, Shah R, O'Regan P, West SC. RAD51C is required for Holliday junction processing in mammalian cells. Science 2004;303:243–6. [PubMed: 14716019]
40. Liu Y, Tarsounas M, O'Regan P, West SC. Role of RAD51C and XRCC3 in genetic recombination and DNA repair. J Biol Chem 2006;282:1973–9. [PubMed: 17114795]

41. Liu X, Holstege H, van der Gulden H, et al. Somatic loss of BRCA1 and p53 in mice induces mammary tumors with features of human BRCA1-mutated basal-like breast cancer. Proc Natl Acad Sci U S A 2007;104:12111–6. [PubMed: 17626182]

42. Frappart PO, Lee Y, Lamont J, McKinnon PJ. BRCA2 is required for neurogenesis and suppression of medulloblastoma. Embo J 2007;26:2732–42. [PubMed: 17476307]

43. Cheung AM, Elia A, Tsao MS, et al. Brca2 deficiency does not impair mammary epithelium development but promotes mammary adenocarcinoma formation in p53(+/−) mutant mice. Cancer Res 2004;64:1959–65. [PubMed: 15026330]

44. Mao JH, Perez-Losada J, Wu D, et al. Fbxw7/Cdc4 is a p53-dependent, haploinsufficient tumour suppressor gene. Nature 2004;432:775–9. [PubMed: 15592418]

45. Ponzone R, Baum M. The BRCA paradox in breast and ovarian cancer. Eur J Cancer 1998;34:966–7. [PubMed: 9849441]

46. Liu B, Parsons R, Papadopoulos N, et al. Analysis of mismatch repair genes in hereditary non-polyposis colorectal cancer patients. Nat Med 1996;2:169–74. [PubMed: 8574961]

47. Rustgi AK. The genetics of hereditary colon cancer. Genes Dev 2007;21:2525–38. [PubMed: 17938238]

48. Mitsumori K, Elwell MR. Proliferative lesions in the male reproductive system of F344 rats and B6C3F1 mice: incidence and classification. Environ Health Perspect 1988;77:11–21. [PubMed: 3289903]

49. Fong LY, Fidanza V, Zanesi N, et al. Muir-Torre-like syndrome in Fhit-deficient mice. Proc Natl Acad Sci U S A 2000;97:4742–7. [PubMed: 10758156]

50. Niemann C, Owens DM, Schettina P, Watt FM. Dual role of inactivating Lef1 mutations in epidermis: tumor promotion and specification of tumor type. Cancer Res 2007;67:2916–21. [PubMed: 17409394]

51. Zurcher M, Hintschich CR, Garner A, Bunce C, Collin JR. Sebaceous carcinoma of the eyelid: a clinicopathological study. Br J Ophthalmol 1998;82:1049–55. [PubMed: 9893597]

52. Lai TF, Huilgol SC, Selva D, James CL. Eyelid sebaceous carcinoma masquerading as in situ squamous cell carcinoma. Dermatol Surg 2004;30:222–5. [PubMed: 14756656]

53. Herschkowitz JI, Simin K, Weigman VJ, et al. Identification of conserved gene expression features between murine mammary carcinoma models and human breast tumors. Genome Biol 2007;8:R76. [PubMed: 17493263]

54. Goldberg M, Rummelt C, Foja S, Holbach LM, Ballhausen WG. Different genetic pathways in the development of periocular sebaceous gland carcinomas in presumptive Muir-Torre syndrome patients. Hum Mutat 2006;27:155–62. [PubMed: 16395674]

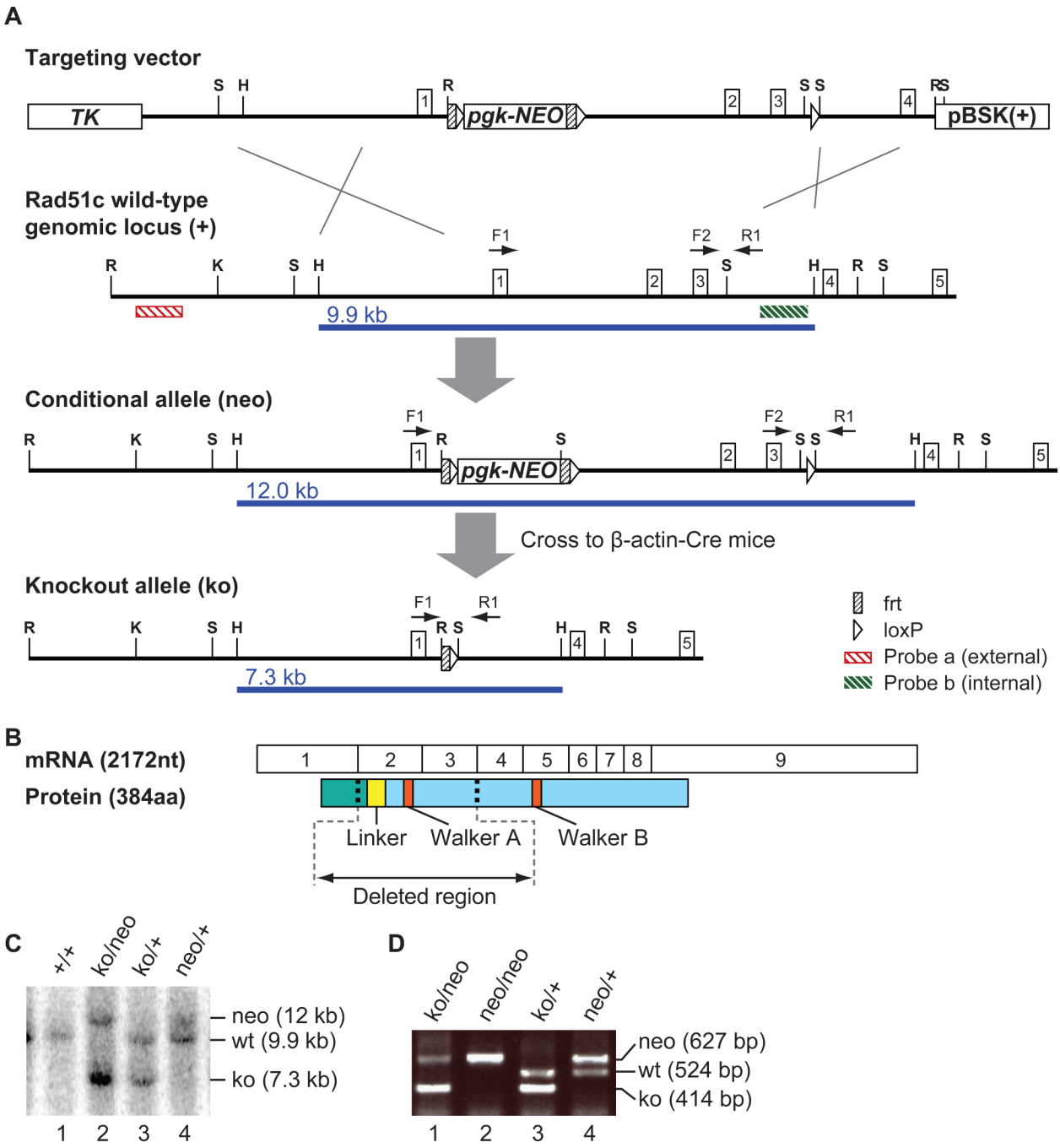

Figure 1. Mouse *Rad51c* gene targeting

(**A**) Scheme illustrating the gene targeting strategy to generate a *Rad51c*-null allele. *Rad51c* exons are indicated as boxes with corresponding numbers. Restriction sites are labeled as S for *Sal*I, H - *Hpa*I, R - *Eco*RI, and K - *Kpn*I. F1, F2, and R1 designate location and direction of primers used for PCR-genotyping. *Hpa*I restriction fragments detected by Southern analysis with the internal probe b are indicated as blue lines under each allele. A *frt-loxP*-PGK-EM7-*neomycin*-bp(A)-*frt-loxP* cassette was targeted into the first intron of *Rad51c (*at genomic location *chr11: 87217150)* and a single *loxP* site was inserted the third intron (at genomic location Chr11: 87214383) (**B**) Depiction of exon structure of the *Rad51c* transcript and the corresponding protein with functionally important regions. N-terminal domain is shown in

green and C-terminal domain in shown in blue. (**C**) Genotyping by Southern blot showing four different genotypes with allele sizes labeled at the right. (**D**) Examples of genotyping using PCR primers shown in (A).

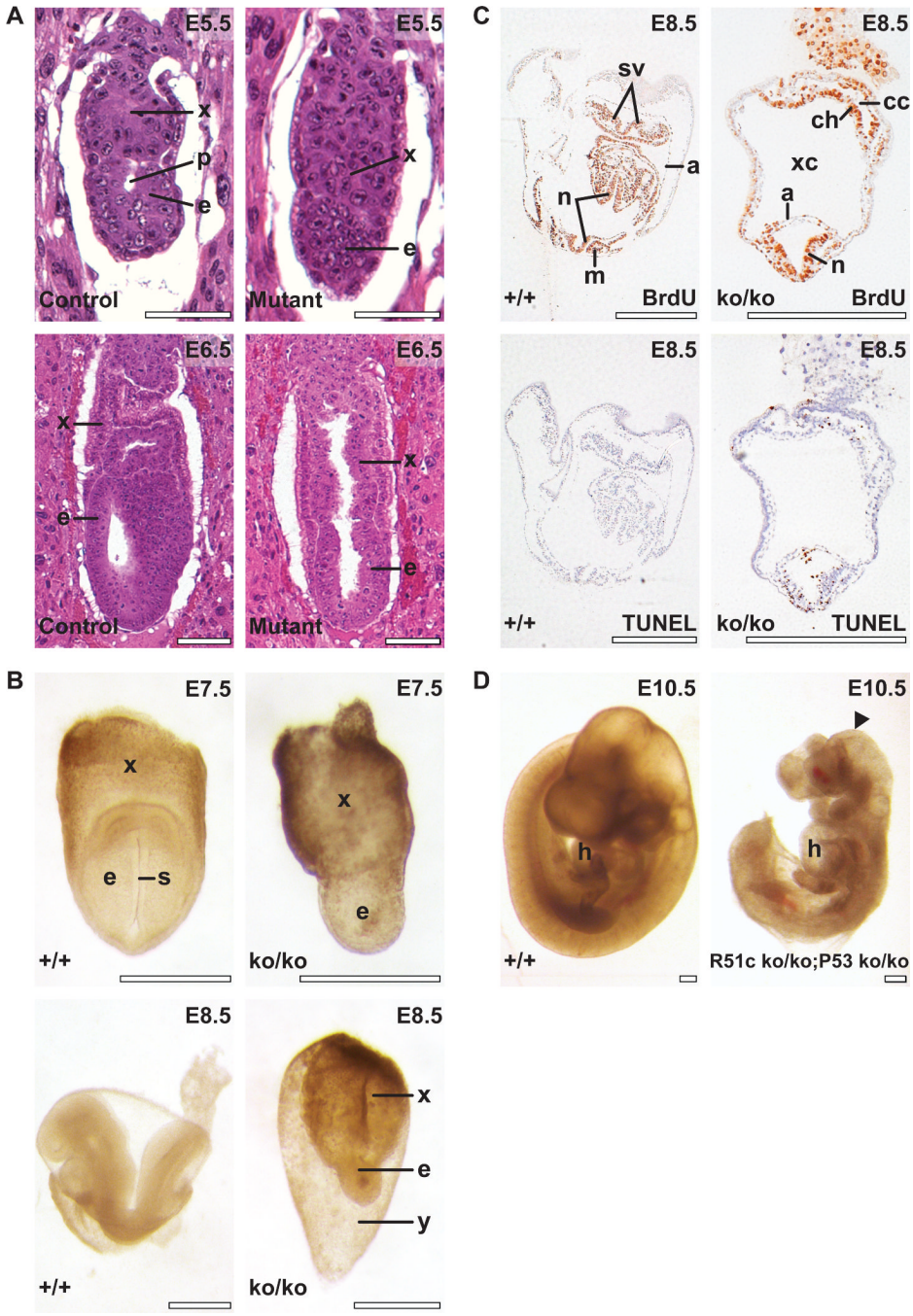

Figure 2. *Rad51c*$^{ko/ko}$ mice die during early embryogenesis

(**A**) Early postimplantation embryos sectioned with the deciduas and stained with hematoxylin and eosin. Top left, developmentally normal control E5.5 embrys reveals equally developed embryonic (e) and extraembryonic (x) tissues with a proamniotic cavity (p) clearly visible. Top right, mutant embryo demonstrates reduced embryonic tissues (e) without the cavity. At E6.5, development of embryonic tissues of the mutant embryo (bottom right) continues to lag behind compared with control embryos (Bottom left). (**B**) control (top left) and mutant (top right) embryos at E7.5. Primitive streak (s) is observed in control embryo. Morphology of control (bottom left) and mutant (bottom right) embryos at E8.5. x and e, as above; y, yolk sac. (**C**) Embryonic tissues in mutant embryo at E8.5 reveal active proliferation as evidenced by BrdU

staining (top right) and increased apoptosis detected by TUNEL assay (bottom right) compared with control littermates (top and bottom left, respectively). n, neural folds; m, somites; a, amnion; sv, sinus venosus; xc, extraembryonic coelomic cavity; ch, prospective chorion; cc, ectoplacental cavity. Scale bar corresponds to 100 μm in A, and to 500 μm in B-D. (**D**) Partial rescue of the *Rad51c*-null phenotype on *Trp53*-deficient genetic background. *Rad51c*$^{ko/ko}$; *Trp53*$^{ko/ko}$ embryo at E10.5 (right) has almost normal morphology but smaller than a control *Rad51c*$^{ko/+}$; *Trp53*$^{ko/+}$ littermate (left). Notice truncated caudal region and unclosed head folds in the mutant embryo (arrowhead). Mutant embryo shows apparently normal looking heart (h).

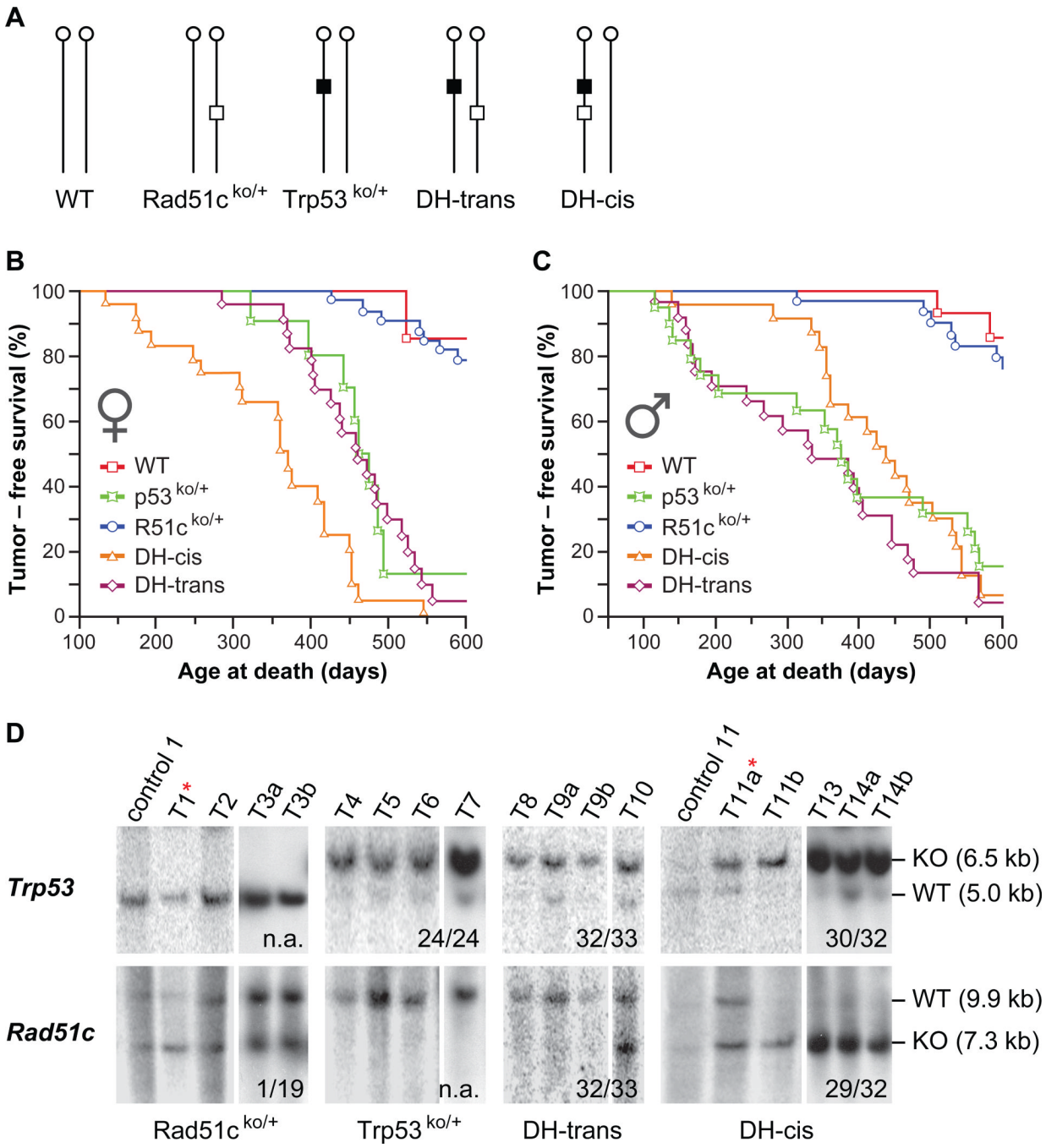

Figure 3. Interaction between *Rad51c* and *Trp53* in mouse tumorigenesis

(**A**) Schematic illustration of the five genotypic mouse cohorts used in the study. Vertical lines with a circle at the top indicate mouse chromosome 11 with a centromere. Open box specifies a mutant *Rad51c* allele. Closed box represents a mutant *Trp53* allele. (**B** and **C**) Kaplan-Meier plot showing tumor-free survival for each group separately for females (B) and males (C). Statistical evaluation of these data is shown in Table 1. (**D**) Southern blot analysis of tumor tissues for LOH at *Trp53* locus (upper panel) and *Rad51c* locus (lower panel). Animal genotype is indicated at the bottom. “T” marks tumor samples T1, sarcoma, NOS, muscle; T2, B-cell Lymphoma; T3a, Pituitary adenoma; T3b Hemangiosarcoma; T4, sarcoma, NOS, muscle; T5 rhabdomyosarcom, muscle; T6, sarcoma, NOS, muscle; T7, mammary adenoma; T8,

rhabdomyosarcoma, muscle; T9a, rhabdomyosarcoma, muscle; T9b, rhabdomyosarcoma, muscle. T10, cholangiosarcoma,liver; T11a, osteosarcoma, vertebra; T11b, myoepitheliaoma, salivary gland; Letters a and b after the tumor number, indicate that the tumors are from the same animal. Control lanes show tail DNA samples for the tumor samples in the following lane. The only tumor from *Rad51c*$^{ko/+}$ animal showing LOH for *Rad51c* and another tumor from *DH-cis* animal showing LOH for *Trp53* but not *Rad51c* is indicated with an asterisk (*) next to tumor number. Faint wild-type bands observed in LOH samples are likely be due to the presence of contaminating normal infiltrating inflammatory cells. Numbers at the bottom of each panel indicate the number of samples showing LOH relative to the total number of tumor samples tested. n.a., not applicable.

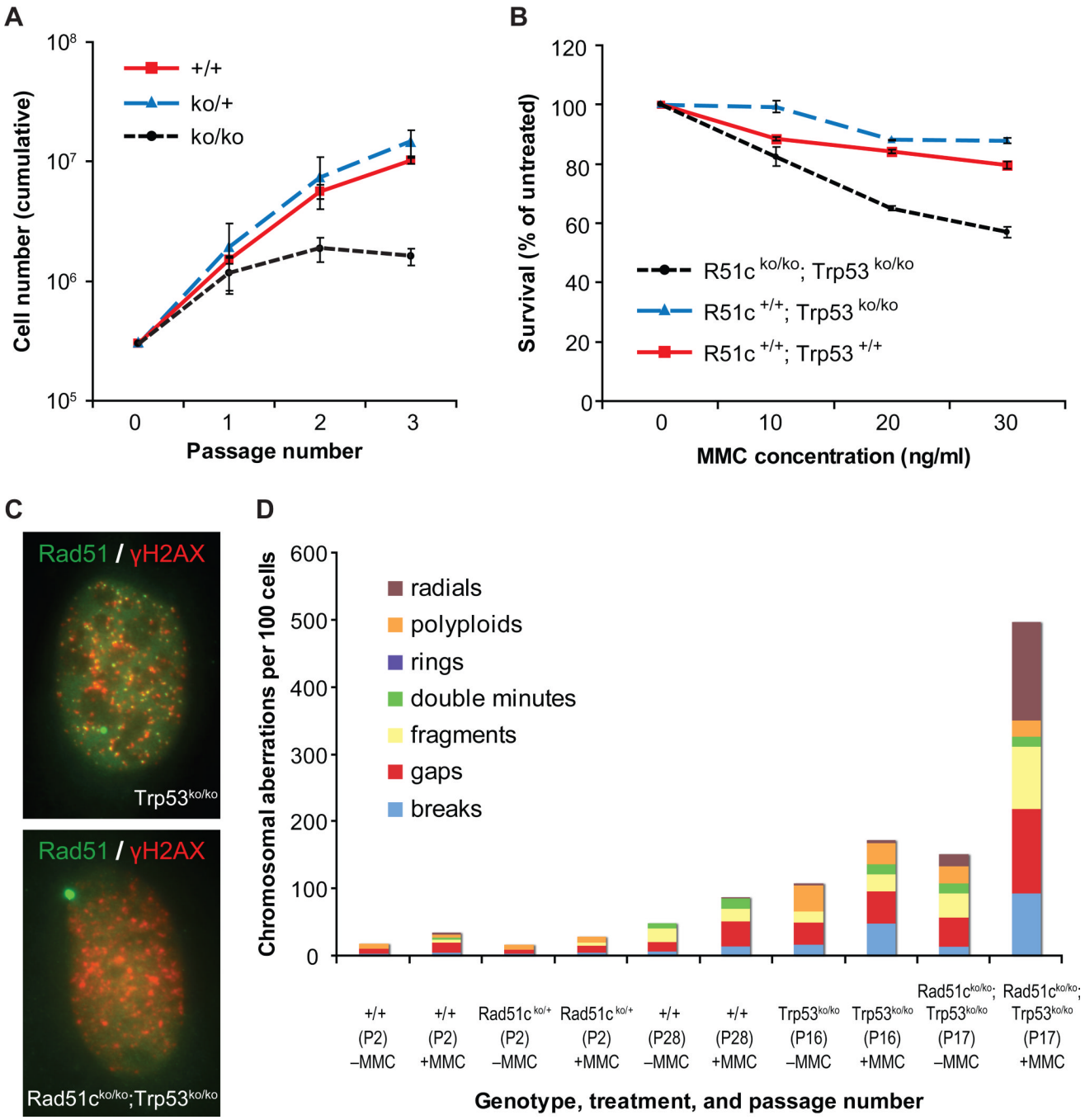

Figure 4. Loss of *Rad51c* results in proliferation defect and genomic instability in MEFs

(**A**) Deletion of *Rad51c* induces growth arrest in primary MEFs. Wild-type, *Rad51c*$^{neo/+}$ or *Rad51c*$^{neo/neo}$ MEFs have been infected with adenovirus carrying *Cre*-recombinase and proliferation has been tested using the 3T3 protocol. (**B**) Sensitivity of MEFs isolated from E10.5 mouse embryos to mitomycin C (MMC). (**C**) *Rad51c*-null MEFs do not form Rad51 foci 6 hours after γ-irradiation (10 Gy). Merged images are shown with Rad51 stained green and γH2AX in red. Genotype of the cell is indicated at the bottom of each image. (**D**) Rad51c-deficient cells accumulate various chromosomal aberrations especially after MMC treatment. The number for each aberration type is depicted proportionally in a stacked bar graph for each

cell line. Genotype, passage number (P) and treatment (+ or − MMC) are indicated below each bar.

Table 1

Tumor-free survival varies with sex and genotype.

Genotype	Gender	Total number of animals	Animals with tumors	Median tumor-free survival time (days)	*P* value* (M vs. F)	Differences between groups*	
WT	F	17	2	> 600	n.a.	n.a.	
Rad51c$^{ko/+}$	F	38	7	> 600	n.a.	vs. *WT*	p=0.4402
Trp53$^{ko/+}$	F	11	8	475	n.a.	n.a.	
DH-trans	F	26	21	461	n.a.	vs. *Trp53*$^{ko/+}$	p=0.8635
DH-cis	F	23	22	360	n.a.	**vs. *Trp53***$^{ko/+}$ **vs. *DH-trans***	**p=0.0030** **p=0.0001**
WT	M	21	3	> 600	0.7839	n.a.	
Rad51c$^{ko/+}$	M	32	6	> 600	0.9765	vs. *WT*	p=0.5499
Trp53$^{ko/+}$	M	20	16	385	0.2345	n.a.	
DH-trans	M	24	22	334	**0.0013**	vs. *Trp53*$^{ko/+}$	p=0.4652
DH-cis	M	24	22	437	**0.0466**	vs. *Trp53*$^{ko/+}$ vs. *DH-trans*	p=0.7757 p=0.0621

P-values were calculated using the Wilcoxon text.

*Statistically significant differences are highlighted in bold.

Table 2

DH-cis mice develop a unique tumor spectrum.

Tumor type	Females			Males		
	Trp53$^{ko/+}$	*DH-trans*	*DH-cis*	*Trp53*$^{ko/+}$	*DH-trans*	*DH-cis*
Osteosarcoma[*]	5 (45%)	11 (42%)	7 (30%)	-	1 (4%)	-
Muscle sarcoma[*]	1 (9%)	-	2 (9%)	11 (55%)	13 (54%)	6 (25%)
Preputial gland carcinoma[†]	-	-	-	-	1 (4%)	10 (42%)
Zymbal's gland carcinoma[†]	-	2 (8%)	-	1 (5%)	-	5 (21%)
Muzzle area carcinomas[†]	-	1 (4%)	4 (17%)	2 (10%)	2 (8%)	5 (21%)
Total number of animals	11	26	23	20	24	24

[*]Tumor types characteristic for *Trp53*$^{ko/+}$ mice

[†]Tumor types characteristic for *DH-cis* mice